Crystallization of Poly(butylene terephthalate)/ Poly(ethylene octene) Blends: Nonisothermal Crystallization

Jiann-Wen Huang,[1] Ya-Lan Wen,[2,3] Chiun-Chia Kang,[4] Mou-Yung Yeh,[5,6] Shaw-Bing Wen[2,3]

[1]*Department of Styling and Cosmetology, Tainan University of Technology, 529 Chung Cheng Road, Yung Kang City 710, Taiwan, Republic of China*
[2]*Department of Nursing, Meiho Institute of Technology, 23 Ping Kuang Road, Neipu Hsiang, Pingtung 912, Taiwan, Republic of China*
[3]*Department of Resources Engineering, National Cheng Kung University, 1 University Road, Tainan City 701, Taiwan, Republic of China*
[4]*R&D Center, Hi-End Polymer Film Company, Limited, 15-1 Sin Jhong Road, Sin Ying City 730, Taiwan*
[5]*Department of Chemistry, National Cheng Kung University, 1 University Road, Tainan City 701, Taiwan, Republic of China*
[6]*Sustainable Environment Research Centre, National Cheng Kung University, Tainan City 701, Taiwan, Republic of China*

Received 4 April 2007; accepted 6 June 2007
DOI 10.1002/app.26960
Published online 24 September 2007 in Wiley InterScience (www.interscience.wiley.com).

ABSTRACT: Poly(ethylene octene) (POE), maleic anhydride grafted poly(ethylene octene) (mPOE), and a mixture of POE and mPOE were added to poly(butylene terephthalate) (PBT) to prepare PBT/POE (20 wt % POE), PBT/mPOE (20 wt % mPOE), and PBT/mPOE/POE (10 wt % mPOE and 10 wt % POE) blends with an extruder. The melting behavior of neat PBT and its blends nonisothermally crystallized from the melt was investigated with differential scanning calorimetry (DSC). Subsequent DSC scans exhibited two melting endotherms ($T_{m\mathrm{I}}$ and $T_{m\mathrm{II}}$). $T_{m\mathrm{I}}$ was attributed to the melting of the crystals grown by normal primary crystallization, and $T_{m\mathrm{II}}$ was due to the melting of the more perfect crystals after reorganization during the DSC heating scan. The better dispersed second phases and higher cooling rate made the crystals that grew in normal primary crystallization less perfect and relatively prone to be organized during the DSC scan. The effects of POE and mPOE on the nonisothermal crystallization process were delineated by kinetic models. The dispersed phase hindered the crystallization; however, the well-dispersed phases of an even smaller size enhanced crystallization because of the higher nucleation density. The nucleation parameter, estimated from the modified Lauritzen–Hoffman equation, showed the same results. J Appl Polym Sci 107: 583–592, 2008

Key words: blends; crystallization; elastomers; kinetics (polym.); melt

INTRODUCTION

Poly(butylene terephthalate) (PBT) is an important thermoplastic material for a large number of applications because of its good combination of properties, such as rigidity and solvent resistance. Its low impact strength can be overcome through blending with some elastomers, such as poly(ethylene octene) (POE),[1–3] poly(acrylonitrile-*co*-butadiene-*co*-styrene),[4–7] ethylene–propylene–diene,[8] ethylene–propylene rubber,[9,10] and poly(ethylene-*co*-glycidyl methacrylate).[11] The toughness and crystallization of PBT depend on the compatibility and interactions between components induced by chemical reactions.

Correspondence to: J.-W. Huang (jw.huang@msa.hinet.net).

Journal of Applied Polymer Science, Vol. 107, 583–592 (2008)

Controlling crystallization is of great importance in polymer processing. Most of the properties of a polymer are affected by the crystalline phase and crystallization rate. The interface between two components is an important factor in crystallization.

In previous research,[12] POE was blended with PBT in an extruder, and the results revealed improved compatibility between PBT and POE in the presence of maleic anhydride grafted poly(ethylene octene) (mPOE). The size of the dispersed phase decreased with an increasing concentration of mPOE and followed the order of PBT/POE > PBT/mPOE/POE > PBT/mPOE. This decrease in the particle size may have been due to improved dispersibility attributable to the reaction of the anhydride groups in mPOE and the OH in PBT at the interface. The addition of POE did not affect the melting behavior of PBT for samples quenched in water after compounding in the extruder. However, differential scanning

calorimetry (DSC) scans of isothermally crystallized neat PBT and PBT blends exhibited two melting endotherms, which were due to melt recrystallization during the DSC scans. The dispersed second phase hindered the crystallization, but the well-dispersed phases of a smaller size enhanced the crystallization because of the higher nucleation density. The equilibrium melting temperature was estimated with the nonlinear Hoffman–Weeks relation. The ranking of the crystallizability of the blends was PBT/mPOE > PBT > PBT/POE > PBT/mPOE/POE on the basis of the same degree of undercooling (ΔT_c) calculated from their respective equilibrium melting temperatures.

Previous research[12] on the polymer crystallization process has been limited to idealized conditions such as isothermal crystallization with constant external conditions; therefore, the theoretical analysis is relatively simple, and problems concerning the cooling rates and thermal gradients within specimens can be avoided. Practically, however, crystallization in a continuously varying environment is of great interest because industrial processes generally proceed under nonisothermal conditions. In this work, the melting behavior of PBT and PBT blends after nonisothermal crystallization was studied with DSC, and several nonisothermal crystallization models were also applied to describe the nonisothermal crystallization process.

EXPERIMENTAL

Materials

Commercial-grade PBT was supplied by Chang Chun Group (Taipei, Taiwan) under the trade name PBT1100-211M with a melt flow index of 18–22 g/10 min (235°C × 2.16 kgf, ASTM D 1238). mPOE with a melt flow index of 1.2 g/10 min (190°C × 2.16 kgf, ASTM D 1238) under the trade name Fusabond MN-493D was produced by DuPont (Wilmington, DE). POE with a melt flow index of 0.5 g/10 min (190°C × 2.16 kgf, ASTM D 1238) was also provided by DuPont (Engage 8150). All materials were used as received without purification.

Sample preparation

All materials were dried at 50°C in a vacuum oven for 6 h before compounding. PBT and 20 wt % POE or mPOE were compounded with a twin-screw extruder (length/diameter = 32, diameter = 40 mm; model CM-MTE 32, Continent Machinery Co., Tainan, Taiwan) at 280°C and 300 rpm to make PBT/POE and PBT/mPOE polymer blends, respectively. A mixture of 10 wt % POE and 10 wt % mPOE was blended with PBT in an extruder to prepare PBT/mPOE/POE. The rod extrudate was cooled in a water bath. For comparison, the neat PBT was also passed through the extruder under the same conditions.

Nonisothermal crystallization

The crystallization behaviors of the polymer blends were investigated with a PerkinElmer DSC-1 differential scanning calorimeter (Waltham, MA). The differential scanning calorimeter was calibrated with indium with samples weights of 8–10 mg. All operations were carried out in a nitrogen atmosphere. Before the data were gathered, the samples were heated to 260°C and held in the molten state for 5 min to eliminate the influence of the thermal history. The sample melts were then subsequently cooled to 35°C at cooling rate (Φ) values of 10, 20, 30, and 40°C/min.

RESULTS AND DISCUSSION

Melting behaviors following nonisothermal crystallization

The crystallization rate has a significant effect on the melting behavior. Figure 1 shows representative DSC heating scans (for the sake of brevity) of PBT/mPOE at a heating rate of 10°C/min after samples were crystallized from 260°C to room temperature with different values of Φ. The determined values of the melting enthalpy ($\Delta H_{m\mathrm{I}}$ and $\Delta H_{m\mathrm{II}}$) related to melting endotherms $T_{m\mathrm{I}}$ and $T_{m\mathrm{II}}$ are also listed in Table I. The DSC scans of all samples displayed two endotherms ($T_{m\mathrm{I}}$ and $T_{m\mathrm{II}}$). The two melting endotherms may be attributed to the melting of crystals with different morphologies[13,14] or to the fact that the crystals have a low degree of perfection and these crystals can partially melt and recrystallize

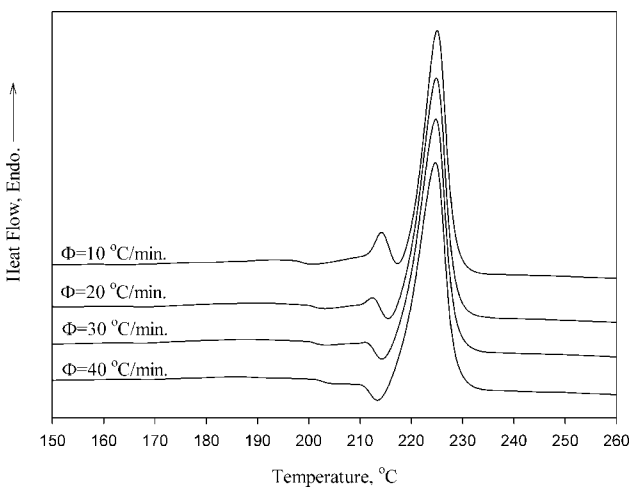

Figure 1 Melting behavior of PBT/mPOE nonisothermally crystallized from the melt with various values of Φ.

TABLE I
DSC Scan Data for PBT, PBT/POE, PBT/mPOE/POE, and PBT/mPOE After Nonisothermal Crystallization

Φ (°C/min)	T_{mI} (°C)	T_{mII} (°C)	ΔH_{mI} (J/g)	ΔH_{mII} (J/g)	$\Delta H_{mI}/\Delta H_{mII}$
PBT					
10	216.4	225.4	5.60	30.81	0.182
20	216.2	225.29	2.81	31.94	0.088
30	215.40	225.17	1.98	35.56	0.056
40	214.54	225.10	1.54	36.53	0.042
PBT/POE					
10	215.8	225.52	5.59	32.80	0.171
20	214.1	224.79	2.66	32.50	0.082
30	213.1	224.68	1.95	35.74	0.055
40	212.7	224.47	1.18	36.63	0.032
PBT/mPOE/POE					
10	214.4	224.4	4.1	40.1	0.102
20	213.2	224.80	1.42	40.54	0.035
30	212.1	224.55	0.59	43.52	0.014
40	211.3	224.57	0.52	45.53	0.011
PBT/mPOE					
10	214.3	224.4	2.4	41.4	0.058
20	212.3	224.8	0.77	40.57	0.019
30	211.2	224.6	0.29	43.58	0.007
40	211.1	224.7	0.24	45.76	0.005

during DSC scans to yield more perfect crystals.[15,16] In previous research,[12] wide-angle X-ray diffraction of all samples exhibited similar patterns and suggested that there were no additional phases resulting in the two melting peaks. The two melting peaks should be T_{mI}, which is associated with the fusion of the crystals grown by normal primary crystallization, and T_{mII}, which is the melting peak of the more perfect crystals after reorganization during the heating process in DSC measurements.[17] Both the shape and position of T_{mI} were influenced by the Φ value of crystallization for all four samples. Table I shows that the position shifted to a lower temperature range and the intensity of T_{mI} decreased with increasing Φ. However, for T_{mII}, their positions remained almost unchanged, and their intensity decreased with an increase in Φ. This indicated that the lower Φ was, the more perfect the crystals were that were grown in normal primary crystallization. When the samples were crystallized at higher Φ values, the formed crystals were less perfect and therefore were relatively prone to be organized during heating into a crystal population with higher thermodynamic stability. However, at lower Φ values, the preexisting crystals were much more perfect and less susceptible to reorganization.[18]

For a specific value of Φ, both T_{mI} and the ratio of ΔH_{mI} to ΔH_{mII} decreased with increasing mPOE content in the blends. As previously studied,[12] the second phases were dispersed better with more mPOE. It seems that the dispersed phases destroyed the crystals that formed in normal primary crystallization and were more susceptible to reorganization.[17,19,20]

Nonisothermal crystallization

Nonisothermal crystallization processes of PBT, PBT/POE, PBT/mPOE/POE, and PBT/mPOE were measured in a Φ range of 10–40°C/min. A representative DSC curve of the PBT/mPOE blend is shown in Figure 2. The onset temperature (T_o) and peak temperature (T_p) of the crystallization exotherms are presented in Table II. In all samples, T_o and T_p shifted to lower temperatures with increasing Φ; the shifting indicated that the lower Φ was, the earlier the crystallization started.

From DSC dynamic crystallization experiments, the data for the crystallization exotherms as a function of temperature were obtained. The relative crystallinity as a function of temperature (X_T) was calculated as the ratio of the exothermic peak areas:[21–23]

$$X_T = \frac{\int_{T_o}^{T} \left[\frac{dH_c}{dT}\right] dT}{\int_{T_o}^{T_\infty} \left[\frac{dH_c}{dT}\right] dT} \quad (1)$$

where T_∞ is the temperature at which crystallization ends, T is an arbitrary temperature and dH_c is the enthalpy of crystallization released during an infinitesimal temperature interval (dT). A representative plot presents X_T as a function of temperature for PBT/mPOE in Figure 3. During the nonisothermal crystallization process, the time (t) and T exhibit the following relationship:

$$t = \left| \frac{T_o - T}{\Phi} \right| \quad (2)$$

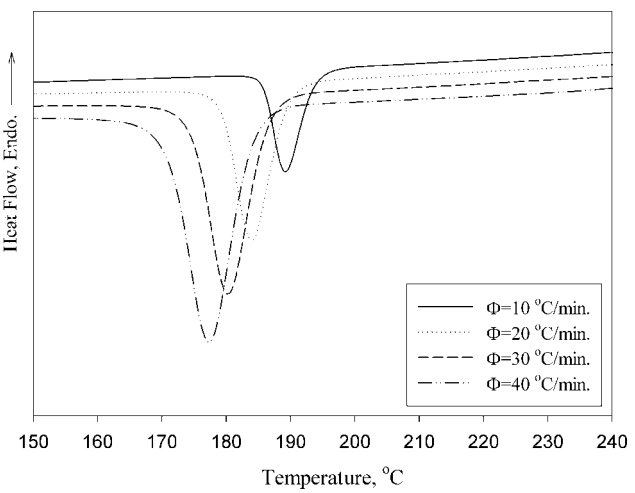

Figure 2 DSC nonisothermal measurement curves for PBT/mPOE.

TABLE II
Characteristic Data for the Nonisothermal Melt Crystallization Exotherms for PBT, PBT/POE, PBT/mPOE/POE, and PBT/mPOE

Φ (°C/min)		10	20	30	40
PBT	T_o (°C)	199.2	196.9	195.6	194.2
	T_p (°C)	191.7	187.7	184.7	182.4
	$t_{1/2}$ (min)	0.706	0.461	0.362	0.295
PBT/POE	T_o (°C)	200.2	198.2	196.5	195.8
	T_p (°C)	194.4	189.3	186.6	183.9
	$t_{1/2}$ (min)	0.662	0.453	0.348	0.274
PBT/mPOE/POE	T_o (°C)	196.6	193.2	191.4	189.2
	T_p (°C)	188.3	182.6	178.4	174.4
	$t_{1/2}$ (min)	0.871	0.557	0.453	0.376
PBT/mPOE	T_o (°C)	197.9	193.5	192.7	189.8
	T_p (°C)	188.3	183.9	181.0	179.6
	$t_{1/2}$ (min)	0.757	0.518	0.391	0.342

The abscissa of the temperature in Figure 3 could be transformed into a timescale. The typical relative crystallinity as a function of time (X_t) is illustrated in Figure 4. At higher Φ values, less time was available to complete the crystallization.

The half-time ($t_{1/2}$) of the nonisothermal crystallization was obtained with the following relationship:

$$t_{1/2} = \left| T_o - T_{1/2} \right| / \Phi \tag{3}$$

where $T_{1/2}$ is the temperature at which X_t is 50%. Table II also shows $t_{1/2}$ for PBT, PBT/POE, PBT/mPOE/POE, and PBT/mPOE. The inverse value of $t_{1/2}$ (i.e., $1/t_{1/2}$) signifies the bulk crystallization rate, and a higher $t_{1/2}$ value (i.e., a lower $1/t_{1/2}$ value) indicates slower crystallization. The $t_{1/2}$ value decreased with increasing Φ, and this indicated that the polymer crystallized more quickly when Φ was increased. The results are discussed in more detail later.

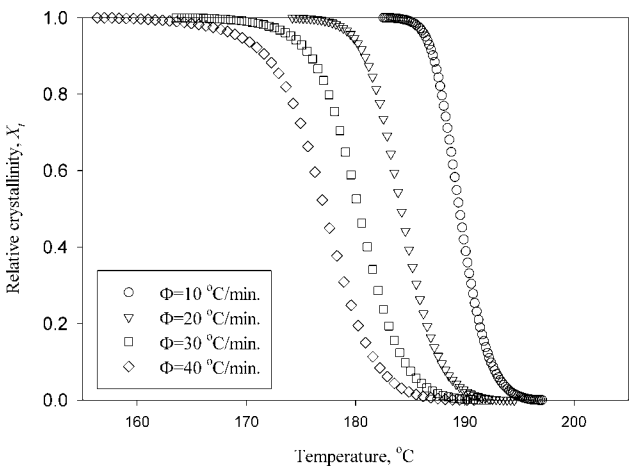

Figure 3 Experimental values of X_t for PBT/mPOE at different values of Φ.

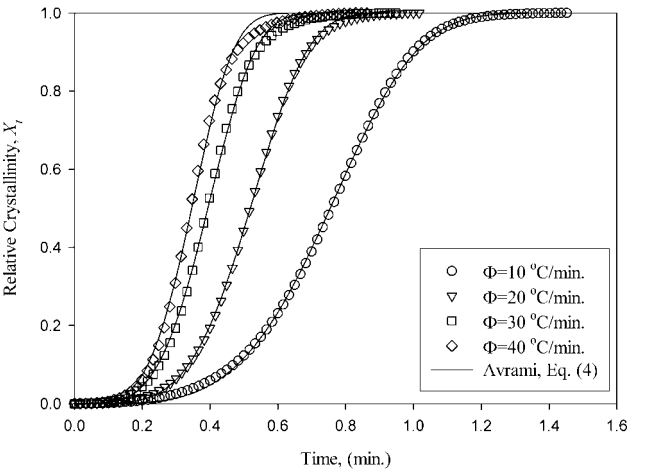

Figure 4 Experimental values of X_t for PBT/mPOE at different values of Φ.

Avrami model

Under the assumption that the crystallization temperature is constant and the thermal lag between the sample and the furnace is kept minimal, the Avrami equation[24–27] can be used to describe the primary stage of nonisothermal crystallization. The Avrami equation is expressed as follows:

$$X_t = 1 - \exp[-(K_a T)^{n_a}] \tag{4}$$

where t is the crystallization time, K_a is the Avrami crystallization rate constant, and n_a is the Avrami exponent. X_t can be calculated as the ratio of the area of the exothermic peak at time t to the total measured area of crystallization. The values of K_a and n_a were determined through the fitting of the experimental data of X_t to eq. (4), and the results are shown in Table III.

In nonisothermal crystallization, K_a and n_a do not have the same physical significance as they do in the isothermal process because the temperature decreases constantly in a nonisothermal process. This temperature changes may affect the rate of both nucleus formation and spherulite growth. However, eq. (4) remains a good fit to experimental data based on the regression coefficient (R^2), as can be seen in Table III. n_a for neat PBT varied from 3.76 to 3.96, suggesting that the crystallization proceeded by thermal nucleation and three-dimensional spherical growth. The n_a values of the three blends were in the range of 3.65–4.35, which indicated that the addition of mPOE or POE apparently did not change the crystallization mechanism of PBT. The n_a values were similar to those reported by Supaphol et al.[28] and Bai et al.,[29] who found n_a values of 3.62–6.17 and 3.5–4.0, respectively, but higher than that reported by Chisholm and Zimmer,[30] who found an

TABLE III
Avrami Kinetic Parameters

Sample	Φ (°C/min)	n_a	K_a	K_J	R^2
PBT	10	3.86	1.2998	1.0266	0.9994
	20	3.96	1.8830	1.0321	0.9997
	30	3.90	2.7018	1.0337	0.9992
	40	3.76	3.9375	1.0349	0.9984
PBT/POE	10	4.03	1.3874	1.0333	0.9998
	20	4.27	2.0146	1.0356	0.9996
	30	4.02	2.9484	1.0367	0.9985
	40	3.97	4.3772	1.0376	0.9987
PBT/mPOE/POE	10	3.44	1.0168	1.0016	0.9990
	20	3.65	1.6039	1.0239	0.9993
	30	3.90	2.217	1.0269	0.9993
	40	3.87	3.0298	1.0281	0.9992
PBT/mPOE	10	4.17	1.2151	1.0197	0.9998
	20	4.35	1.6258	1.0245	0.9998
	30	4.00	2.3199	1.0284	0.9993
	40	4.02	3.1377	1.0290	0.9987

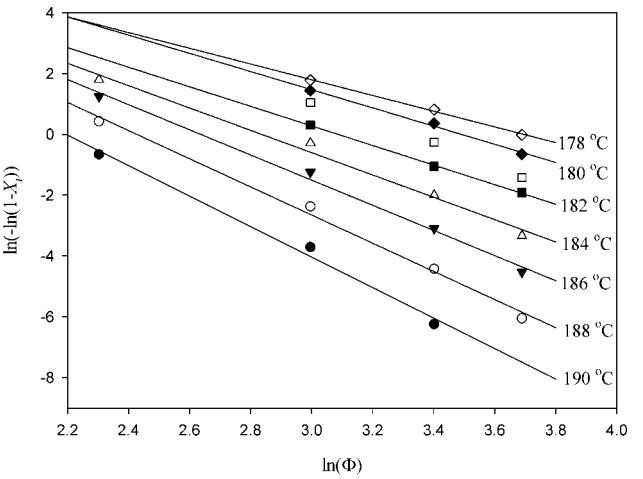

Figure 5 Ozawa analysis based on the nonisothermal crystallization of PBT/mPOE.

average n_a value of 2.48. The differences in the n_a values may be a reflection of memory effects associated with the processing of polymers[31] or different molecular weights.[30]

To meet the requirements of the Avrami model, Jeziorny[32] assumed constant or approximately constant Φ values and proposed the final form of the parameter characterizing the kinetics of a nonisothermal crystallization process:

$$\ln K_J = \frac{\ln K_a}{\Phi} \tag{5}$$

The values of K_J are listed in Table III. K_J increased with increasing Φ for all samples.

Ozawa model

Ozawa[33,34] extended the isothermal Avrami theory to the nonisothermal case by assuming that crystallization occurs at a constant value of Φ, and he provided the following equation:

$$X_T = 1 - \exp\left[-\left(\frac{K_o}{\Phi^{n_o}}\right)\right] \tag{6}$$

where K_o and n_o are the Ozawa crystallization rate constant and Ozawa exponent, respectively. Figure 5 illustrates a typical plot of $\ln[-\ln(1 - X_t)]$ as a function of ln Φ for a fixed temperature. n_o and K_o could be estimated from the slope and y intercept [(K_o = exp(y intercept/n_o)]. The Ozawa kinetic parameters as well as R^2 are listed in Table IV. n_o ranged from 2.03 to 4.00 for neat PBT within 180–194°C, from 2.07 to 4.49 for PBT/POE within 182–194°C, from 1.82 to 5.66 for PBT/mPOE/POE within 174–190°C, and from 3.14 to 4.72 for PBT/mPOE within 178–190°C. n_o decreased as the crystallization temperature decreased, and this indicated that the nucleation mechanism was more instantaneous in time with decreasing temperature during the crystallization process.[35,36] K_o decreased with increasing temperature,

TABLE IV
Ozawa Kinetic Parameters

Sample	Temperature (°C)	n_o	K_o	R^2
PBT	180	2.03	47.4499	0.9998
	182	2.44	36.5444	0.9978
	184	2.79	28.9326	0.9926
	186	2.99	22.3331	0.9902
	188	3.04	16.8417	0.9925
	190	3.33	12.5103	0.9992
	192	3.61	9.2633	0.9975
	194	4.00	6.9500	0.9958
PBT/POE	182	2.07	44.912	0.9982
	184	2.61	34.0985	0.9974
	186	3.02	26.6549	0.9933
	188	3.33	20.8851	0.9776
	190	3.40	15.2495	0.9841
	192	4.04	11.3759	0.9940
	194	4.49	8.6383	0.9971
PBT/mPOE/POE	174	1.82	42.9713	0.9898
	176	2.02	33.1236	0.9901
	178	2.55	25.9749	0.9968
	180	2.91	19.0138	0.9585
	182	3.32	15.6096	0.9589
	184	3.83	13.1715	0.9714
	186	4.48	11.3411	0.9792
	188	4.60	9.3239	0.9945
	190	5.66	7.9858	0.9829
PBT/mPOE	178	3.14	33.1980	0.9881
	180	3.21	27.7045	0.9915
	182	3.29	21.9157	0.9993
	184	3.48	18.3276	0.9700
	186	3.84	14.0123	0.9928
	188	4.32	11.0415	0.9961
	190	4.72	8.7073	0.9946

and this suggested that PBT, PBT/POE, PBT/mPOE/POE, and PBT/mPOE crystallized more slowly with increasing temperature.

Liu model

Liu et al.[37] combined the Avrami [eq. (4)] and Ozawa [eq. (6)] models to deal with nonisothermal crystallization behavior, and its form can be presented as follows:

$$\ln \Phi = \ln\left[\frac{K_o}{K_a^{n_a}}\right]^{\frac{1}{n_o}} - \frac{n_a}{n_o}\ln t \tag{7a}$$

$$F(T) = \left[\frac{K_o}{K_a^{n_a}}\right]^{\frac{1}{n_o}} \tag{7b}$$

$$a = \frac{n_a}{n_o} \tag{7c}$$

where the kinetic parameter, $F(T)$, refers to the value of Φ chosen at the unit crystallization time when the measured system has a certain degree of crystallinity and a is the ratio of n_a to n_o. At a given degree of crystallinity, plotting ln Φ versus ln t yielded a linear relationship between ln Φ and ln t, and the values of $F(t)$ and a (Table V) were obtained from the slopes and intercepts of these lines, respectively. A representative plot of PBT/mPOE is shown in Figure 6. The value of a varied from 1.53 to 1.71 for neat PBT, from 1.62 to 1.69 for PBT/POE, from 1.61 to 1.72 for PBT/mPOE/POE, and from 1.72 to 1.78 for PBT/mPOE. That the value of $F(T)$ increased with an increasing degree of crystallinity indicates that at the unit crystallization time, a higher value of Φ was required to reach a higher degree of crystallinity.

Ziabicki analysis

Ziabicki[38–40] suggested that the kinetics of polymer phase transformation could be described by a first-order kinetic equation:

$$\frac{dX_t}{dt} = K_z(1 - X_t) \tag{8}$$

where K_z is a temperature-dependent crystallization rate function. Ziabicki suggested a concept of kinetic crystallinity:

$$G = \int_{T_g}^{T_m} K_z \, dT \tag{9}$$

The kinetic crystallizability (G) characterizes the degree of crystallinity obtained when the polymer is cooled at the unit Φ value from the melting temperature (T_m) to the glass-transition temperature (T_g). Jeziorny[32,41] derived a simple equation to calculate G:

$$G = \int_{T_g}^{T_m} K_z \, dT = \left(\frac{\pi}{\ln 2}\right)^{1/2} K_{z,\max}\frac{D}{2} \tag{10}$$

where $K_{z,\max}$ is the value of K_z at the maximum crystallization rate and D is the half-width of the crystallization curve.

In nonisothermal crystallization, crystallization rate function K_z is replaced with a derivation function of the relative crystallinity, $(dX/dT)_\Phi$, that is specific for each value of Φ. Equation (10) is replaced by[32]

$$G_\varphi = \int_{T_g}^{T_m} (dX/dT)_\Phi \, dT = \left(\frac{\pi}{\ln 2}\right)^{1/2} (dX/dT)_{\Phi,\max}\frac{D_\Phi}{2} \tag{11}$$

where $(dX/dT)_{\Phi,\max}$ is the maximum crystallization rate and D_Φ is the half-width of the derivative relative crystallinity as a function of temperature. G_Φ is the kinetic crystallizability at an arbitrary value of Φ. The values of D_Φ, $(dX/dT)_{\Phi,\max}$, and G_Φ of all samples are listed in Table V. Because of the effect of Φ, G_Φ must be corrected properly as follows:

TABLE V
Values of $F(T)$ and a for PBT, PBT/POE, and PBT/mPOE

Sample	X_t	$F(T)$	a	R^2
PBT	0.2	3.27	1.71	0.9939
	0.3	4.24	1.65	0.9993
	0.4	5.03	1.62	0.9994
	0.5	5.73	1.61	0.9994
	0.6	6.86	1.53	0.9995
	0.7	7.42	1.56	0.9996
	0.8	7.90	1.64	0.9997
PBT/POE	0.2	3.17	1.69	0.9894
	0.3	4.02	1.65	0.9914
	0.4	4.64	1.63	0.9928
	0.5	5.06	1.62	0.9937
	0.6	5.88	1.62	0.9893
	0.7	6.42	1.63	0.9950
	0.8	7.14	1.66	0.9954
PBT/mPOE/POE	0.2	4.90	1.72	0.9981
	0.3	5.88	1.69	0.9973
	0.4	6.87	1.68	0.9977
	0.5	7.85	1.67	0.9979
	0.6	8.93	1.65	0.9981
	0.7	10.24	1.63	0.9982
	0.8	11.98	1.61	0.9984
PBT/mPOE	0.2	3.81	1.76	0.9954
	0.3	4.74	1.73	0.9965
	0.4	5.52	1.72	0.9972
	0.5	6.25	1.72	0.9977
	0.6	6.97	1.72	0.9980
	0.7	7.74	1.73	0.9983
	0.8	8.47	1.78	0.9983

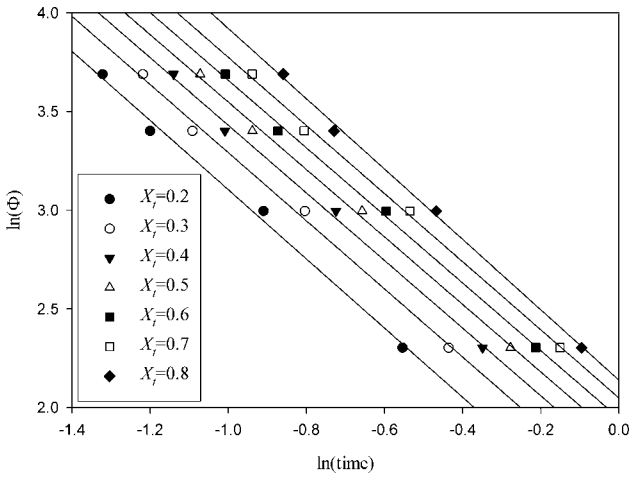

Figure 6 Plots of ln Φ versus ln t for different values of X_t for PBT/mPOE.

$$G_c = \frac{G_\Phi}{\Phi} \tag{12}$$

After the normalization of the effect of Φ, the values of the kinetic crystallizability with the unit cooling (G_c) are shown in Table VI.

Comparison of the kinetic models

The prediction according to the Avrami model is reconstructed in Figure 4. From the comparison of the model prediction with experimental data and the values of the R^2 parameter summarized in Tables III, it is clear that the Avrami model provides a simple method to describe a nonisothermal crystallization process, although the physical meanings of its kinetic parameters (K_a and n_a) are not clear in nonisothermal crystallization because of a continuously changing temperature. n_a contains information on nucleation and growth geometry. The interpretation of the exponent is complicated by factors such as volume changes due to changes in the temperature, phase transformation, incomplete crystallization, annealing, and different mechanisms involved during the process.[24,42]

Ozawa used a quasi-isothermal method to account for the effect of Φ on dynamic crystallization by modifying the Avrami equation. The Ozawa method for the results of crystallization during continuous cooling can be compared with those obtained by means of the Avrami equation under isothermal conditions. Similar to n_a, n_o depends on the nucleation and growth mechanisms. However, the values of n_o are not constant for various temperatures, as shown in Table IV. This may be due to the fact that the X_T value chosen at a given temperature includes the values at the earliest stage and the values from the end stage of crystallization due to the variation in Φ. The crystallization is nucleation-controlling in the early stage of crystallization, and the crystallization rate is lowered by spherulite impingement and secondary crystallization in the end stage of crystallization. The Ozawa model does not seem suitable for neat PBT and PBT blends.

The Liu model combines the Avrami and Ozawa models, and the physical meaning of rate parameter $F(T)$ refers to the necessary value of Φ to reach a defined degree of crystallinity at the unit crystallization time. The good linearity of the plots (ln R against ln t) verifies the advantage of the combined approach.

The Ziabicki model provides the possibility of determining crystallization rates over the whole temperature range of the crystallization process and proposes that the nonisothermal process can be viewed as a sequence of isothermal steps.[42] The practical meaning of G_c in the Ziabicki treatment is to characterize the ability of a polymer to crystallize when it is cooled from T_m to T_g at a unit value of Φ. A higher G_c value indicates that the polymer crystallizes more readily.

All the kinetic parameters from these models [K_J, K_o, $F(T)$, and G_c] predicted that the crystallization rate would follow the order of PBT/POE > PBT >

TABLE VI
Characteristic Data for the Nonisothermal Melt Crystallization Kinetics for PBT, PBT/POE, and PBT/mPOE Based on Ziabicki's Analysis

Φ (°C/min)	10	20	30	40
PBT				
D_Φ (°C)	4.53	5.59	6.13	6.66
$(dX/dT)_{\Phi,max}$	2.00	3.13	4.23	5.06
G_Φ	17.04	32.95	48.96	63.51
G_c	1.70	1.65	1.63	1.59
T_{max} (°C)	191.7	187.3	184.4	182.3
PBT/POE				
D_Φ (°C)	4.19	5.10	5.90	6.27
$(dX/dT)_{\Phi,max}$	2.22	3.48	4.41	5.46
G_Φ	17.53	33.54	49.10	64.66
G_c	1.75	1.68	1.64	1.62
T_{max} (°C)	193.2	188.9	186.0	183.9
PBT/mPOE/POE				
D_Φ (°C)	5.60	7.08	8.06	9.17
$(dX/dT)_{\Phi,max}$	1.50	2.35	3.10	3.62
G_Φ	15.88	31.42	47.10	62.64
G_c	1.59	1.57	1.57	1.57
T_{max} (°C)	188.1	182.2	177.9	174.5
PBT/mPOE				
D_Φ (°C)	4.58	5.71	6.91	7.73
$(dX/dT)_{\Phi,max}$	1.85	2.99	3.72	4.43
G_Φ	16.02	32.18	48.48	64.56
G_c	1.60	1.61	1.62	1.61
T_{max} (°C)	189.1	183.8	180.2	177.1

T_{max} is the maximum temperature.

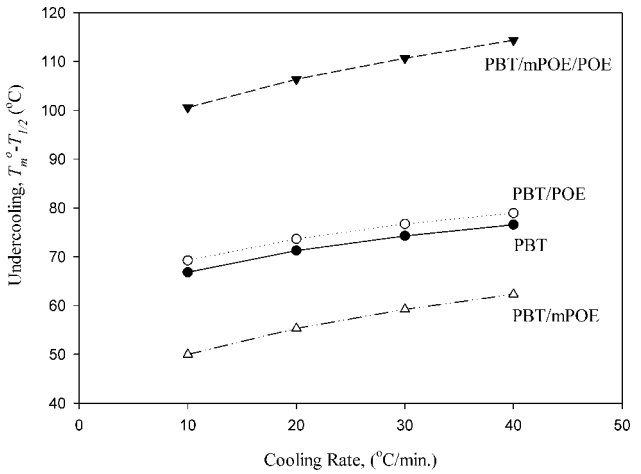

Figure 7 Undercooling to reach 50% relative crystallinity.

PBT/mPOE > PBT/mPOE/POE at a given value of Φ during the nonisothermal crystallization. However, to compare the crystallization ability, the undercooling should be taken into consideration because the crystallization rate of a polymer depends mainly on its undercooling,[42] and the samples have different values of the equilibrium temperature (T_m^o).[12] In a previous study,[12] the T_m^o values of these four samples were estimated with the nonlinear Hoffman–Weeks equation (i.e., T_m^{oNLHW}), and the values were 259.0, 262.8, 288.5, and 239.5°C for PBT, PBT/POE, PBT/mPOE/POE, and PBT/mPOE, respectively. In this article, we try to use the undercooling needed to be imposed to reach 50% relative crystallization ($X_T = 0.5$), that is, $T_m^{oNLHW} - T_{1/2}$, to determine the crystallization ability. Figure 7 shows the undercooling needed to be imposed to reach 50% relative crystallization at different values of Φ. The undercooling followed the order of PBT/mPOE < PBT < PBT/POE < PBT/mPOE/POE, and it indicated that the crystallization ability followed the order of PBT/mPOE > PBT > PBT/POE > PBT/mPOE/POE.

Nadkarni et al.[43] compared nonisothermal experimental data in terms of ΔT_c, which is defined as the temperature difference between the melting peak temperature in the heating scan and the temperature at the onset of crystallization in the cooling scan. However, the undercooling should be calculated as the difference between the equilibrium melting temperatures, where available, and the onset crystallization temperature.[42] The variation of ΔT_c with Φ is shown in Figure 8, and the data can be fitted to a linear equation:

$$\Delta T_c = T_m^o - T_o = P\Phi + \Delta T_c^o \tag{13}$$

where intercept ΔT_c^o signifies the inherent crystallizability of the polymer, being the degree of supercooling required in the limit of zero Φ, and slope P is a process sensitivity factor. The values of ΔT_c^o for PBT, PBT/POE, PBT/mPOE/POE, and PBT/mPOE were 58.4, 61.4, 89.8, and 39.2°C, respectively, suggesting that the crystallization ability followed the order of PBT/mPOE > PBT > PBT/POE > PBT/mPOE/POE. The order was similar to that obtained from $T_m^{oNLHW} - T_{1/2}$. The overall crystallization ability is governed by nucleation and diffusion.[44] The maleic anhydride groups of mPOE might associate through some interactions such as hydrogen bonding to form effective nuclei to enhance crystallization.[45] The dispersion phase would hinder the crystallization by slowing down the diffusion of PBT chains (in PBT/POE and PBT/mPOE/POE); however, the well-dispersed phases of an even smaller size (in PBT/mPOE) would produce more nuclei and induce a higher nucleation density to enhance crystallization. Similar phenomena have been reported in the literature.[46]

Lauritzen–Hoffman equation

Lim et al.[47] modified the Lauritzen–Hoffman equation to measure the spherulite growth rate as a function of temperature and Φ in nonisothermal crystallization as follows:

$$\ln G + \frac{U^*}{R(T_o - \Phi t - T_\infty)} = \ln G_o - \frac{K_g}{(T_o - \Phi t)[T_m^o - (T_o - \Phi t)]f} \tag{14a}$$

$$f = \frac{2(T_o - \Phi t)}{T_m^o + (T_o - \Phi t)} \tag{14b}$$

where G is the growth rate and is approximated as $1/t_{1/2}$ (i.e., $t = t_{1/2}$); G_o is the pre-exponential factor;

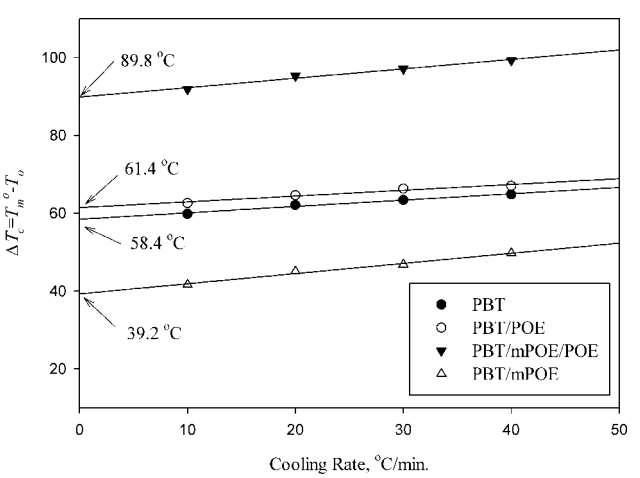

Figure 8 Plot of ΔT_c as a function of Φ.

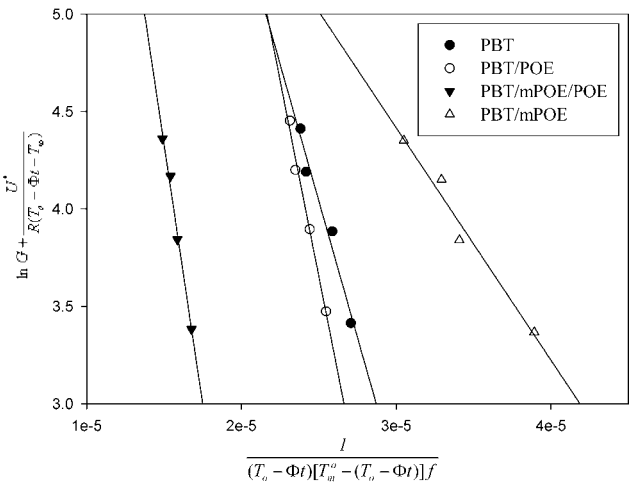

Figure 9 Plot of $\ln G + \frac{U^*}{R(T_o - \Phi t - T_\infty)}$ as a function of $\frac{1}{(T_o - \Phi t)[T_m^o - (T_o - \Phi t)]f}$ according to the modified Lauritzen–Hoffman equation.

U^* is the diffusional activation energy for the transport of crystallizable segments at the liquid–solid interface; R is the gas constant; $T_\infty = T_g - 30°C$ is the hypothetical temperature below which viscous flow ceases; T_g is the glass-transition temperature of PBT ($-25°C$);[48] and K_g is the nucleation parameter, which can be related to the product of the lateral and folding surface free energies. Figure 9 shows a linear plot of eq. (9) for PBT, PBT/POE, and PBT/mPOE with $T_m^o = T_m^{oNLHW}$. K_g was obtained from the slope of Figure 9, and the values were 2.81×10^5, 4.02×10^5, 5.34×10^5, and 1.19×10^5 K^2 for PBT, PBT/POE, PBT/mPOE/POE, and PBT/mPOE, respectively. Comparing the corresponding values of K_g with those values obtained from isothermal crystallization in a previous study,[12] we found that the values of K_g showed the following trend: PBT/mPOE/POE > PBT/POE > PBT > PBT/mPOE. The higher values of K_g for the PBT/POE and PBT/mPOE/POE blends than for neat PBT indicated that the presence of dispersed POE reduced the mobility of polymer chains during crystallization. The more dispersed POE in the PBT/mPOE blend caused more heterogeneous nucleation and a lower value of K_g.

CONCLUSIONS

The melting behavior of neat PBT, PBT/POE, PBT/mPOE/POE, and PBT/mPOE nonisothermally crystallized from the melt with various values of Φ was investigated with DSC. Subsequent DSC scans of nonisothermally crystallized samples exhibited two melting endotherms that were due to the melt–recrystallization process. The lower temperature ($T_{m\mathrm{I}}$) was associated with the fusion of the crystals grown by normal primary crystallization, and the higher one ($T_{m\mathrm{II}}$) was the melting peak of the more perfect crystals after reorganization during the DSC heating process. The more dispersed second phases (with a higher content of mPOE) and higher Φ values made the crystals grown in normal primary crystallization less perfect and relatively prone to be organized during the DSC scan. The nonisothermal crystallization process of PBT and its blends were delineated by modified Avrami, Ozawa, Liu, Ziabicki, and Nadkarni models. The Avrami model provided the best method to describe the crystallization, although the physical meanings of its kinetic parameters (K_a and n_a) are not clear. It is appropriate to compare the crystallization ability with the Nadkarni model, in which ΔT_c was considered because the crystallization rate of a polymer depends mainly on its undercooling. The trend of the crystallization rate in a lower undercooling range was as follows: PBT/mPOE > PBT > PBT/POE > PBT/mPOE/POE. However, the crystallization ability followed this order: PBT/mPOE > PBT > PBT/POE > PBT/mPOE/POE. The dispersion phase hindered the crystallization; however, the well-dispersed phases of an even smaller size (PBT/mPOE) enhanced crystallization because of the higher nucleation density. K_g, estimated from the modified Lauritzen–Hoffman equation, showed the same trend.

References

1. Aróstegui, A.; Gaztelumedi, M.; Nazábal, J. Polymer 2001, 42, 9565.
2. Guerrica-Echevarria, G.; Eguiazabal, J. I.; Nazabal, J. Polym Eng Sci 2006, 46, 172.
3. Aróstegui, A.; Nazábal, J. Polym Eng Sci 2003, 43, 1691.
4. Hale, W.; Keskkula, H.; Paul, D. R. Polymer 1999, 40, 365.
5. Hale, W.; Keskkula, H.; Paul, D. R. Polymer 1999, 40, 3665.
6. Hale, W. R.; Pessan, L. A.; Keskkula, H.; Paul, D. R. Polymer 1999, 40, 4237.
7. Hale, W.; Lee, J. H.; Keskkula, H.; Paul, D. R. Polymer 1999, 40, 3621.
8. Wang, H. X.; Zhang, H. X.; Wang, Z. G.; Jiang, B. Z. Polymer 1997, 38, 1569.
9. Cecere, A.; Greco, R.; Ragosta, G.; Scarinzi, G.; Taglialatela, A. Polymer 1990, 31, 1239.
10. Vongpanish, P.; Bhowmick, A. K.; Inoue, T. Plast Rubber Comp Proc Appl 1994, 21, 109.
11. Aróstegui, A.; Nazábal, J. J Polym Sci Part B: Polym Phys 2003, 41, 2236.
12. Huang, J. W.; Wen, Y. L.; Kang, C. C.; Yeh, M. Y.; Wen, S. B. J Appl Polym Sci, to appear.
13. Roberts, R. C. Polymer 1969, 10, 113.
14. Roberts, R. C. Polymer 1969, 10, 117.
15. Yeh, J. T.; Runt, J. J Polym Sci Part B: Polym Phys 1989, 27, 1543.
16. Nichols, M. E.; Robertson, R. E. J Polym Sci Part B: Polym Phys 1992, 30, 305.
17. Liu, X.; Li, C.; Zhang, D.; Xiao, Y. J Polym Sci Part B: Polym Phys 2006, 44, 900.
18. Wang, Y.; Bhattacharya, M.; Mano, J. F. J Polym Sci Part B: Polym Phys 2005, 43, 3077.

19. Kalkar, A. K.; Deshpande, A. A. Polym Eng Sci 2001, 41, 1597.
20. Srimoaon, P.; Dangseeyun, N.; Supaphol, P. Eur Polym J 2004, 40, 599.
21. Hay, J. N.; Sabir, M. Polymer 1969, 10, 203.
22. Hay, J. N.; Fitzgerald, P. A.; Wiles, M. Polymer 1976, 17, 1015.
23. Hay, J. N. Br Polym J 1979, 11, 137.
24. Wunderlich, B. Macromolecular Physics; Academic: New York, 1976; Vol. 2.
25. Avrami, M. J. Chem Phys 1939, 7, 1103.
26. Avrami, M. J. Chem Phys 1940, 8, 212.
27. Avrami, M. J. Chem Phys 1941, 9, 177.
28. Supaphol, P.; Dangseeyun, N.; Srimoaon, P. Polym Test 2004, 23, 175.
29. Bai, H.; Zhang, Y.; Zhang, Y.; Zhang, X.; Zhou, W. J Appl Polym Sci 2006, 101, 1295.
30. Chisholm, B. J.; Zimmer, J. G. J Appl Polym Sci 2000, 76, 1296.
31. Fornes, T. D.; Paul, D. R. Polymer 2003, 44, 3945.
32. Jeziorny, A. Polymer 1978, 19, 1142.
33. Ozawa, T. Polymer 1971, 12, 150.
34. Apiwanthanakorn, N.; Supaphol, P.; Nithitanakul, M. Polym Test 2004, 23, 817.
35. Supaphol, P.; Spruiell, J. E. J Appl Polym Sci 2000, 75, 337.
36. Janeschitz-Kriegl, H.; Ratajski, E.; Wippel, H. Colloid Polym Sci 1999, 277, 217.
37. Liu, T. X.; Mo, Z. S.; Wang, S. E.; Zhang, H. F. Polym Eng Sci 1997, 37, 568.
38. Ziabicki, A. Colloid Polym Sci 1974, 252, 433.
39. Ziabicki, A. J Chem Phys 1968, 48, 4368.
40. Ziabicki, A. Appl Polym Symp 1967, 6, 1.
41. Supaphol, P. J Appl Polym Sci 2000, 78, 338.
42. DiLorenzo, M. L.; Silvestre, C. Prog Polym Sci 1999, 24, 917.
43. Nadkarni, V. M.; Bulakh, N. N.; Jog, J. P. Adv Polym Technol 1993, 12, 73.
44. Fatou, J. G. Makromol Chem 1984, 7, 131.
45. Seoa, Y.; Kima, J.; Kima, K. U.; Kimb, Y. C. Polymer 2000, 41, 2639.
46. Zhang G.; Yan, D. J Appl Polym Sci 2003, 88, 2181.
47. Lim, B. A.; McGuire, K. S.; Lloyd, D. R. Polym Eng Sci 1993, 33, 537.
48. Cheng, S. Z. D.; Pan, R.; Wunderlich, B. Makromol Chem 1988, 18, 2443.